Environ Sci Pollut Res (2016) 23:14422–14430
DOI 10.1007/s11356-016-6588-2

RESEARCH ARTICLE

Efficient photocatalytic degradation of tetracycline hydrochloride by Ag_3PO_4 under visible-light irradiation

QiShe Yan[1] · MengMeng Xu[1] · CuiPing Lin[1] · JiFei Hu[1] · YongGang Liu[1] · RuiQin Zhang[1]

Received: 4 January 2016 / Accepted: 28 March 2016 / Published online: 11 April 2016

Abstract A facile, environmental-friendly Ag_3PO_4-PN photocatalyst was synthesized by a simple precipitation method at room temperature in the presence of ammonia and polyvinyl pyrrolidone (PVP). As-synthesized samples were characterized by scanning electron microscopy (SEM), X-ray diffraction (XRD), X-ray photoelectron spectroscopy (XPS), and UV–visible diffuse reflectance spectroscopy (UV–vis DRS). The enhancement of photocatalytic efficiency of Ag_3PO_4-PN is strongly dependent on the excellent photo-absorption capacity, sharp edges and corners, and synergistic effect of PVP and $NH_3{\cdot}H_2O$. The effects of catalyst dosage, TC concentration and solution pH were explored with tetracycline hydrochloride (TC) as target contamination. The mineralization was evaluated by total organic carbon (TOC) analysis and determination of the concentration of inorganic ions such as NO_3^- and Cl^-. Radical detection experiment indicated the h^+ and $\cdot O^{2-}$ are major active species in the degradation of TC by Ag_3PO_4-PN. Moreover, photocatalyst stability and regeneration experiments exhibited the favorable stability and rejuvenation ability, suggesting a promising prospect of practical application of Ag_3PO_4 in the wastewater treatment.

Keywords Photocatalytic reaction · Ag_3PO_4 · Tetracycline hydrochloride · Radical detection · Catalyst regeneration

Responsible editor: Philippe Garrigues

✉ QiShe Yan
yanqishezzu@163.com

[1] College of Chemistry and Molecular Engineering, Zhengzhou University, Zhengzhou 450001, China

Introduction

As a "green" technology, semiconductor photocatalysis has been widely used for the treatment of water polluted by organic dye [Mahmoodi et al. 2011; Xiao et al. 2012]. TiO_2 was one of the most widely researched photocatalyst, with the advantages of non-toxicity, high stability, low-cost. Unfortunately, TiO_2 can only utilize the ultraviolet ray consisting of about 5 % of the solar spectrum due to the relatively wide band gap and the high recombination rate, which seriously confine the photocatalysis performance and practical application of TiO_2 [Katsumata et al. 2013]. From the view of using solar light for environmental remediation, exploring more efficient visible-light-induced photocatalysts has attracted considerable attention.

In recent years, silver orthophosphate (Ag_3PO_4) is being thoroughly investigated by increasing researchers, because of excellent photocatalytic performance and efficient separation of photoexcited electrons and holes. Ag_3PO_4 exhibited extremely excellent oxidative capacities for the evolution of O_2 from water, as well as the degradation of organic dyes under the solar irradiation [Yi et al. 2010]. It was reported by Bi et al., that the shape and facet effects of Ag_3PO_4 crystals on their photocatalytic properties, where the photocatalytic performance of single-crystalline Ag_3PO_4 rhombic dodecahedrons with only {110} facets exposed was much higher than that of cubes bounded entirely by {100} facets, ascribing to the higher surface energy of {110} facets [Bi et al. 2011]. In addition, other researchers successfully synthesized different shapes of Ag_3PO_4 single crystals, such as the cubes [Yang et al. 2014], tetrapods [Wang et al. 2013], myriapods [Teng et al. 2015; Wang et al. 2014c], branches [Li et al. 2014; Wang et al. 2014a], and spherical nanocrystals [Liu et al. 2014]. In spite of high efficiency of Ag_3PO_4 previously reported, the self-corrosion and bad stability always limit the application

of Ag_3PO_4 photocatalyst. Therefore, it becomes very important for Ag_3PO_4 to successful regeneration.

As a type of wide pollutant, the pharmaceuticals and personal care products (PPCPs) are focused on increasing concern by scientists [Daughton and Ternes 1999; Ellis 2006; Ternes et al. 2004]. Among these, antibiotics are widely used for human and animal health, which are paid more comprehensive attention than other PPCPs [Golovko et al. 2014; Ortiz de Garcia et al. 2014].

In general, the Ag_3PO_4 photocatalysis degradation under visible-light irradiation of organic pollutants has mainly been applied to colored dyes, including methylene blue, rhodamine B, and methyl orange [Hua et al. 2015], while few reports have focused on antibiotics compounds [Wang et al. 2015; Wu et al. 2013].

As the second most usage of antibiotics, tetracycline (TC) has been used as broad-spectrum antibacterial agent for human and animal health, leading to a large amount of residual in aquatic and soil environment, which in turn threatened human health for appearance of drug-resistant bacteria and clinical side effects on liver and kidney [Martins et al. 2014]. Therefore, it is essential to exploit cost-efficient and feasible treatment technologies to remove these contaminations in the aquatic environment.

In this paper, we successfully prepared high-efficiency, micron-scale polyhedral Ag_3PO_4-PN photocatalyst with sharp corners and edges with the synergetic assistances of PVP and $NH_3{\cdot}H_2O$. The catalysts were characterized by a series of methods. In this paper, tetracycline hydrochloride (TC), a kind of common broad-spectrum antibiotics, was selected as the target pollutant. Then, we investigated the photocatalysis performance and mineralization capacity of TC by as-synthesized Ag_3PO_4-PN. Moreover, the photocatalytic reaction mechanism, photocatalyst stability, and regeneration of obtain Ag_3PO_4-PN were also surveyed.

Experimental

Materials and methods

All the reagents used were of analytical purity and were used without further purification. Silver nitrate ($AgNO_3$), disodium hydrogen phosphate dodecahydrate ($Na_2HPO_4 \cdot 12H_2O$) and ammonium oxalate (AO) were purchased from Tianjin Kermel Chem. Reagent Co., Ltd. Polyvinyl pyrrolidone (PVP, Mw 58000, K 29–32) was purchased from Shanghai Aladdin BioChem. Tech. Co., Ltd. Ammonia solution ($NH_3{\cdot}H_2O$) was purchased from Luoyang Chem. Reagent Factory. Benzoquinone (BQ) and t-butyl alcohol (TBA) were Flukaimport reagents subpackaged by Shanghai Chemical Dispensing Factory and Shanghai Asus Fine Chemical Co., Ltd. Hydrogen peroxide (H_2O_2 30 %) was purchased by Tianjin Fengchuan Chemical Reagent Technologies Co., Ltd.

In a typical synthesis, 0.2 g PVP was added in 300 ml deionized water with continuous stirring for 10 min. 0.6 g $AgNO_3$ was dissolved in the above solution and stirred for 20 min in darkness. Ammonia solution (1:1, *v:v*) was added until solution became clear, then continuously stirred for 10 min. Then 50 ml, 0.15 M Na_2HPO_4 solution was added drop-by-drop to above mixture solution, and stirred for 4 h. The yellow precipitate was centrifuged and washed with deionized water and absolute ethanol for several times and dried at 60 °C for 12 h and was designed as Ag_3PO_4-PN. And three similar procedures were used to prepare Ag_3PO_4 without the presence of PVP, $NH_3{\cdot}H_2O$, PVP, and $NH_3{\cdot}H_2O$, and were designed as Ag_3PO_4-N, Ag_3PO_4-P, and Ag_3PO_4-A, respectively.

Characterization

X-ray diffraction (XRD) analysis was performed on an X-ray diffractometer (X'Pert PRO MRD, PANalytical, the Netherlands) equipped with a Cu Kα X-ray source. The morphology of the samples was investigated by scanning electron microscopy (SEM, Quonxe-2000, Philips, the Netherlands). The surface elemental component and the chemical state of the sample were analyzed by X-ray photoelectron spectroscopy (XPS, PHI 5300, Perkin Elmer) with a monochromatized Al Kα X-ray source ($h\nu = 1487$ eV). UV–vis diffuse reflection spectra (UV–vis DRS) of the samples were obtained using a UV–vis spectrophotometer (Caly 5000, Agilent, USA). The band gap energy (Eg) of these samples was evaluated using the following equation [Guan et al. 2013; Liang et al. 2012]:

$$\alpha(h\nu) = A\left(h\nu - E_g\right)^2 \quad (1)$$

where α, ν, E_g, and A are the absorption coefficient, light frequency, band gap energy, and a constant, respectively [Yi et al. 2010].

Measure of photocatalytic activity

The as-prepared photocatalyst activity was measured by the degradation of TC. A 100 mg photocatalyst was added to 50 mL of contamination solution as the initial concentration was 30 mg/L. Before illumination, the solution with a certain amount of photocatalyst was stirred for 30 min in darkness to reach the adsorption and desorption equilibrium. A 420-nm filter was placed between xenon lamp and reaction solution to filter ultraviolet. And the experimental device was illustrated in Fig. 1. At the process of the illumination of 350 W xenon lamp, a specified volume of solution was fetched at a given

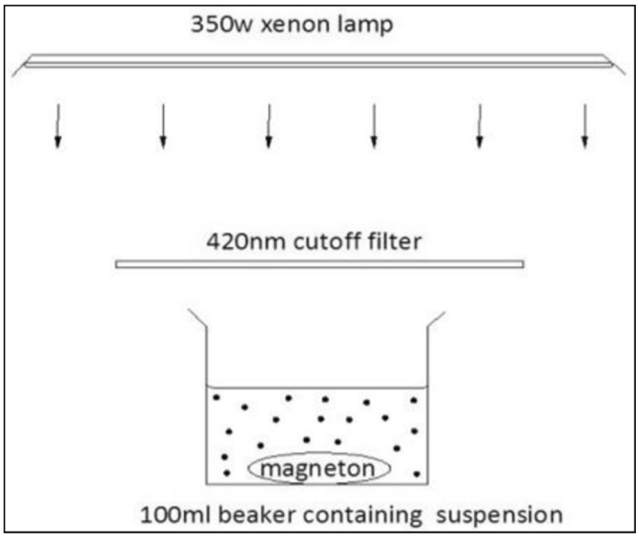

Fig. 1 The illustration of photocatalysis experiment device

time interval and filtered immediately with 0.45 μm membrane filter. The concentration of TC solution were evaluated by UV–vis spectroscopy (UV-2450, Shimadzu, Japan), with 357.5 nm of the maximum absorption wavelength. The degradation efficiency was calculated by 1-c/c_0, while the c was instantaneous concentration and c_0 was solution concentration after adsorption process. The data of degradation experiment was the average value of three times parallel experiments. And the standard deviations of the average of independent runs are all between 1.2 and 2.9 %.

The mineralization degree of TC and residual of long-lived organic intermediates in the solutions [Zhang et al. 2013] were measured by total organic carbon (TOC). The TOC concentration of filtrate was determined by using Total Organic Carbon Analyzer (TOC-$V_{CPH/CPN}$, Shimadzu, Japan). The NO_3^- and Cl^- concentrations of TC solution were determined by ion chromatograph (IC), equipped with anion chromatography column (AS-14), anion guard column (AG-14), chemical suppressor (AMMS 30), and 8.0 mM Na_2CO_3/1.0 mM $NaHCO_3$ as a leacheate with 0.8 mL min^{-1} of flow rate and dilute sulphuric acid as regeneration solution.

Detection of reactive oxygen species

The scavenging experiments of reactive oxygen species were similar to the photodegradation experiments. Different quantity of scavengers was added into the TC solution prior to addition of catalysts. These experiments were carried out according to the previous study [Lin et al. 2012]. The concentrations of scavengers were 1×10^{-3} mol/L (7.2 mg), 1.6×10^{-2} mol/L (0.1 g), and 1×10^{-3} mol/L (5.4 mg) for TBA, AO, and BQ, respectively. The concentration of solution was also measured by solution absorbance using a spectrophotometer (Shimadzu UV-2450).

Results and discussion

Characterization of photocatalysts

Crystal structure

The X-ray diffraction (XRD) patterns of Ag_3PO_4 samples (Fig. 2) show that all the diffraction peaks of the samples could be indexed to the body-centered cubic structure of Ag_3PO_4 (JCPDS card No. 06-0505). No peaks assignable to other phases are observed, indicating a high purity of Ag_3PO_4 samples. The sharp and strong diffraction peaks indicate that the Ag_3PO_4 catalysts were well crystallized. In addition, the peak intensity of Ag_3PO_4-N and Ag_3PO_4-PN are stronger than those of Ag_3PO_4-A and Ag_3PO_4-P, indicating the addition of $NH_3 \cdot H_2O$ is in favor of formation of crystals.

In order to investigate the valence states and surface chemical compositions of the Ag_3PO_4-PN microstructure, XPS analysis was employed and the results are shown in Fig. 3. Figure 3a presents an overview of the XPS spectrum of pure Ag_3PO_4-PN microstructures. Ag, P, O, and adventitious C coexist in the Ag_3PO_4-PN microstructures. Figure 3b–d display the high resolution XPS spectra of Ag, P, and O, respectively. In Fig. 3b, the peaks centered at 373.7 and 367.7 eV are ascribed to Ag $3d_{3/2}$ and $3d_{5/2}$, respectively, revealing the Ag exists mainly in the +1 oxidation state in the sample. As shown in Fig. 3c, the peak of P 2p is located at 132.5 eV, indicating that the oxidation state of P is +3 in the sample [Bertrand 1981]. In addition, the spectrum of O 1 s is located at 530.4 eV, which is assigned to the O_2^- in Ag_3PO_4 [Katsumata et al. 2014].

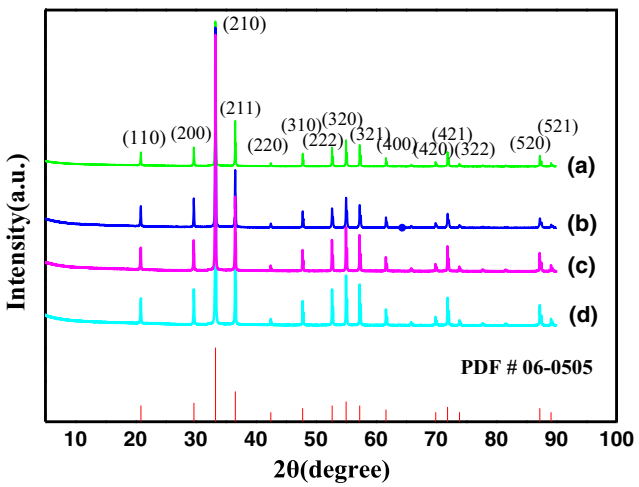

Fig. 2 XRD patterns of different Ag_3PO_4 powers: **a** Ag_3PO_4-A; **b** Ag_3PO_4-P; **c** Ag_3PO_4-N; **d** Ag_3PO_4-PN

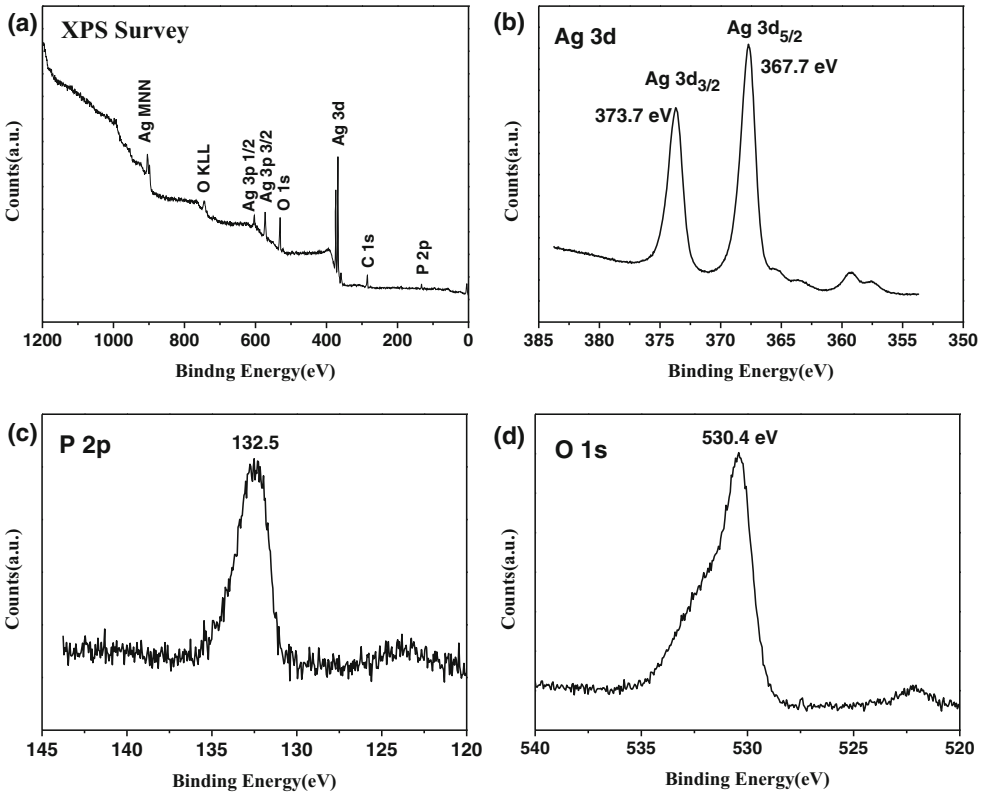

Fig. 3 **a** Overview XPS spectrum of Ag_3PO_4-PN microstructure, **b**–**d** are the XPS spectra of Ag_3PO_4-PN microstructure for the Ag 3d spectrum, P 2p spectrum, and O 1 s spectrum

Crystal morphology

The morphology and size of the Ag_3PO_4 samples were surveyed by SEM. Figure 4a reveals the as-synthesized Ag_3PO_4-A is constituted of quasi-spherical particles with diameters around 600 nm. Figure 4b shows the quasi-tetrahedron morphology of Ag_3PO_4-P due to the addition of PVP as the structure inducer with the size in the range of 1–10 μm. Ag_3PO_4-N has a cube structure with the size of 2–10 μm (Fig. 4c), while Ag_3PO_4-PN exhibited a polyhedron structure with the size of 0.5–7 μm (Fig. 4d). The formation of sharp edges and corners on the surfaces of cube and polyhedron may be benefit from the introduction of $NH_3{\cdot}H_2O$ [Guo et al. 2015].

Optical property

The optical property of Ag_3PO_4 samples was measured by UV–vis DRS, and the UV–vis spectra are exhibited in Fig. 5. The four samples are all Ag_3PO_4 prepared only with different additives, so the optical absorption edges of the samples have rarely significant difference and it is largely related to electronic structure of materials. It can be clearly seen that all the Ag_3PO_4 samples display photo-absorption in the UV and visible region. The absorption edges of Ag_3PO_4-A and Ag_3PO_4-PN are ca. 530 nm, while those of Ag_3PO_4-P and Ag_3PO_4-N are ca. 550 nm, which have slight shift to red. It is noted that the absorbance of Ag_3PO_4-P sample is obviously lower than those of Ag_3PO_4-A, Ag_3PO_4-N, and Ag_3PO_4-PN samples in the range of 330–500 nm, which may adverse to degradation performance of Ag_3PO_4-P sample.

Photocatalytic activity

Comparison of degradation activity of four Ag_3PO_4 catalysts

The photocatalytic activities of the four Ag_3PO_4 samples were tested by photodegradation of TC under visible-light irradiation and the results are shown in Fig. 6a. The Ag_3PO_4-PN exhibited the highest degradation efficiency, arriving 91 % after 120 min of visible-light irradiation. The degradation efficiencies of TC by Ag_3PO_4-A, Ag_3PO_4-P, and Ag_3PO_4-N are 78, 72, and 85 %, respectively. The degradation of TC by Ag_3PO_4 under visible-light irradiation followed pseudo-second-order kinetics and the reactive rate constants of four Ag_3PO_4 samples are 0.0006, 0.0009, 0.0013, 0.0023 L mg^{-1} min^{-1}, respectively, which are shown in Fig. 6b. The higher degradation efficiencies of Ag_3PO_4-N and Ag_3PO_4-PN are attributed to generation of smooth surface, sharp edges and corners, which might contribute to the photocatalysis process at the surface owing to [100] plane with high surface energies [Bi et al. 2011; Guo et al. 2015]. The enhanced photocatalytic activity of Ag_3PO_4-PN benefits from the synergistic effect of

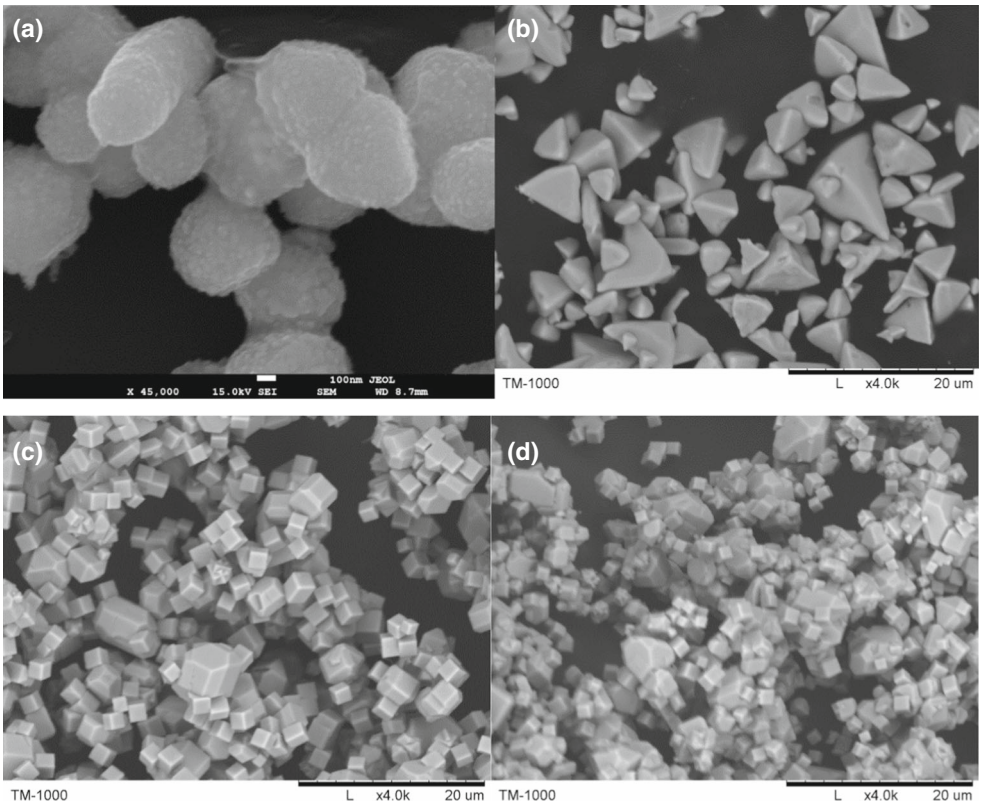

Fig. 4 SEM of the obtained Ag_3PO_4 samples: **a** Ag_3PO_4-A; **b** Ag_3PO_4-P; **c** Ag_3PO_4-N; **d** Ag_3PO_4-PN

PVP and $NH_3 \cdot H_2O$ which not only inhibits the crystal aggregation but also facilitates the order array of crystals. Besides, the strong visible-light absorption capacity and appropriate particle sizes of Ag_3PO_4-PN are also conducive to the improvement of photocatalytic activity. The lowest degradation efficiency of Ag_3PO_4-P is by reason of low absorbance in visible region, which is consistent with results in Fig. 5.

Effect of the reaction conditions

Since the enhanced photocatalytic activity, Ag_3PO_4-PN was selected to degrade contamination in the later experiments. To investigate the effects of various reaction conditions on the photocatalytic efficiency of tetracycline hydrochloride (TC), three reaction conditions were researched, including catalyst dosage, TC concentration, and pH of TC solution. The catalyst dosage was ranged from 0.25 to 3.0 g/L. The result shows that the degradation efficiency of TC increased with the increase of catalyst dosage, while it barely continuously rose until catalyst dosage increasing to 2 g/L (Fig. 7a). It has been reported that in a certain dosage range, radicals increases with the increase of catalyst dosage owing to the increase of the generated carriers [Bertelli and Selli 2004]. But the scatter reflection will result in a low utilization of irradiation light because of an over dosage [Wang et al. 2014b]. To take both into account, the dosage of 2 g/L is used in the later experiments. The effect of TC concentration on the photocatalytic efficiency of TC was investigated (Fig. 7b) with the range of 20–60 mg/L. The results exhibited that the degradation efficiency of TC by Ag_3PO_4-PN increased with the solution concentration up to 30 mg/L, and then decreased with the increase of TC concentration. The effect of pH of TC solution on the photocatalytic efficiency of TC was also investigated (Fig. 7c). The result indicates that the photocatalytic efficiencies of TC under weak acid and neutral conditions were higher than those under strong acid and alkaline conditions, which may because of instability of Ag_3PO_4 photocatalyst under strong acid and alkaline conditions. From above conclusion, the degradation efficiency of TC by Ag_3PO_4-PN was highest

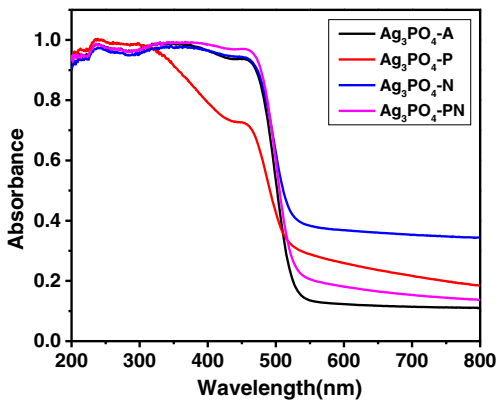

Fig. 5 UV–vis DRS of prepared Ag_3PO_4 samples

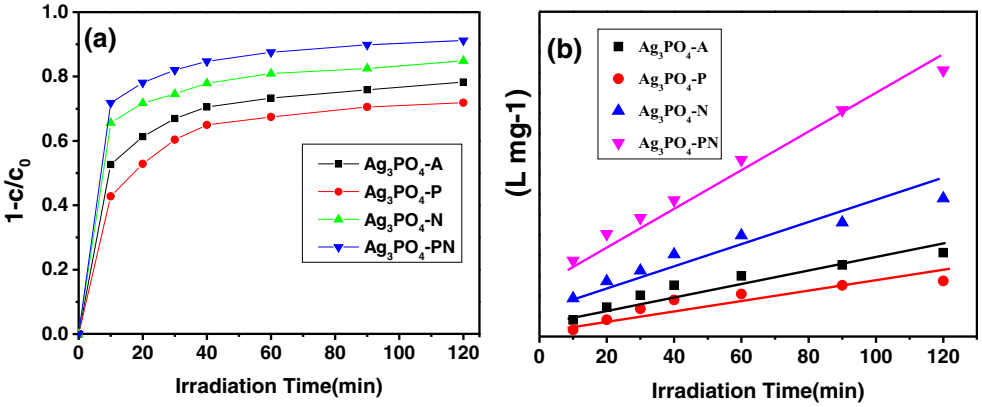

Fig. 6 Photocatalytic degradation efficiency (**a**) and degradation kinetic fitting (**b**) of different Ag_3PO_4 samples under solar irradiation with the 2.0 g L^{-1} of catalyst concentration and 30 mg L^{-1} of initial concentration of TC

with 2 g/L of catalyst dosage, 30 mg/L of TC concentration, and 5 of pH of TC solution.

Photocatalytic degradation mechanism

TOC and IC

Total organic carbon (TOC) was frequently applied as an important index to represent the concentration of organic matter in contamination solution [Sakthivel et al. 2003]. Herein, the mineralization of TC is evaluated by TOC content and quantitative determination of inorganic ions by Ag_3PO_4-PN as the photocatalyst. Figure 8a shows TOC removal increases with increase in irradiation time and arrived *ca.* 45 % through consecutive irradiation of visible light at 120 min. Moreover, due to the presence of nitrogen and chlorine elements, the detection of inorganic ions was also used to assess the mineralization degree of TC. The quantity measurements of NO_3^- and Cl^- were carried out by IC during the photodegradation process (Fig. 8b). The Cl^- concentration of TC solution rapidly decreases during dark adsorption process, which may by reason of the generation of AgCl. With the increase of irradiation time, the Cl^- concentration remains drop, owing to the catalytic oxidization. In addition, the NO_3^- concentration showed

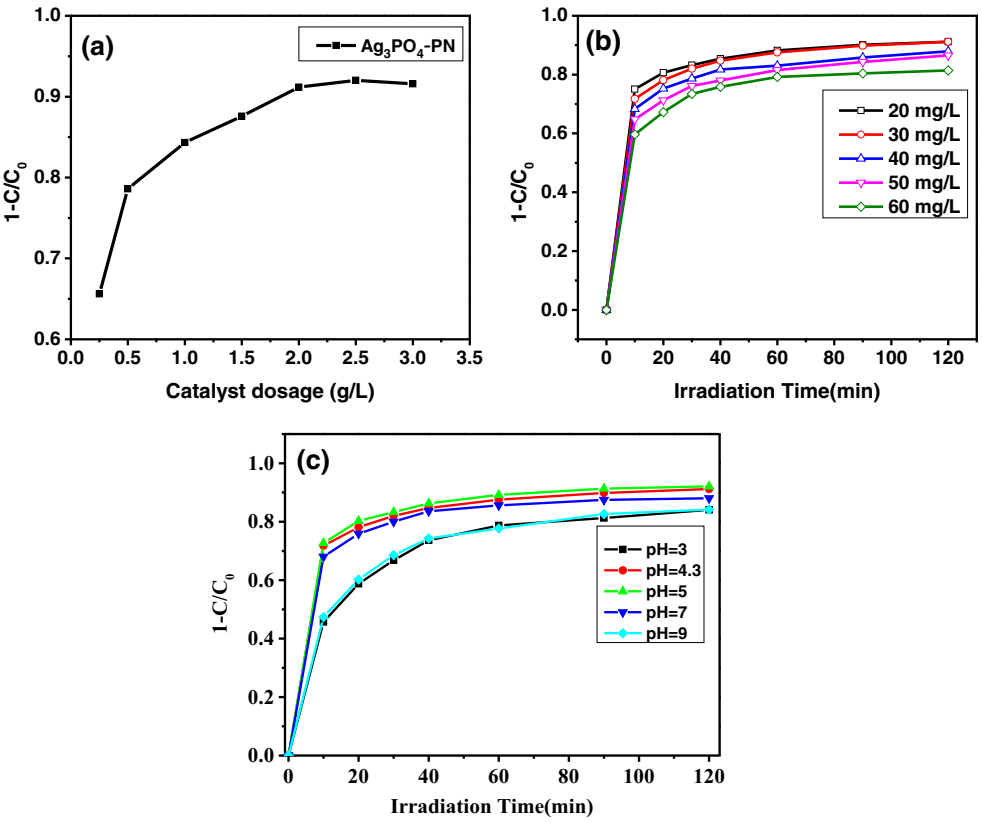

Fig. 7 Effects of the Ag_3PO_4-PN dosage (**a**), TC concentration (**b**) and pH of TC solution (**c**) on the degradation efficiencies of TC under visible-light irradiation, with irradiation for 120 min

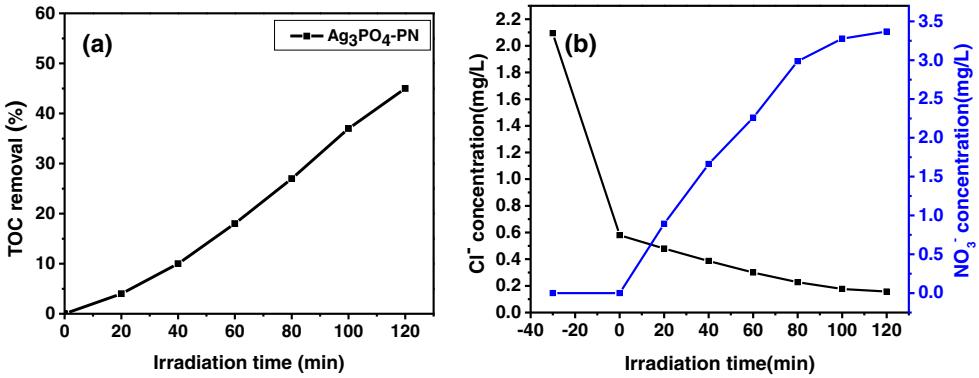

Fig. 8 TOC removal (**a**) and Cl^- and NO_3^- concentration (**b**) of TC solution vs. irradiation time with TC concentration of 30 mg/L and Ag_3PO_4-PN dosage of 2 g/L

a gradually increased tendency with the illumination irradiation, indicating the nitrogen of TC molecular was partly oxidized into NO_3^-. Previous studies [Bandara et al. 1997] have demonstrated the conversion of intermediate nitrite partly into ammonia and nitrate. The formation of NH_3 which escapes may account for the loss of nitrogen in the mass balance.

Oxidative radical species

To investigate the photocatalytic mechanism of Ag_3PO_4-PN into more detail, the effects of active species scavengers on the degradation of TC were examined to shed light on the predominant reactive oxygen species in the photocatalytic process (Fig. 9). In this study, AO, BQ, and TBA were added into the reaction solution as h^+, $\cdot O^{2-}$, and ·OH scavenger, respectively [Lin et al. 2012]. Without the addition of the scavengers, the photocatalytic efficiency of TC is 91 % after 120 min of visible-light irradiation. As is clear from Fig. 9, the addition of TBA scarcely affected the degradation efficiency of TC by Ag_3PO_4-PN, which indicates that ·OH does not appear to be the main reactive oxygen species in the photocatalytic process of TC by Ag_3PO_4-PN.

The visible-light photocatalytic degradation of TC was significantly inhibited by BQ with 23 % of reduction of degradation efficiency, confirming that $\cdot O^{2-}$ indeed plays an important role in the degradation of TC by Ag_3PO_4-PN. Besides, the addition of AO likewise suppresses the photocatalytic degradation of TC with 19 % of decrease of degradation efficiency. It is, therefore, most likely that the photoinduced holes, with a high oxidation potential of +2.45 V vs. NHE, directly react with organic compounds [Yi et al. 2010]. Therefore, it may be concluded that h^+ and $\cdot O^{2-}$ are major active species in the photodegradation of TC by Ag_3PO_4-PN.

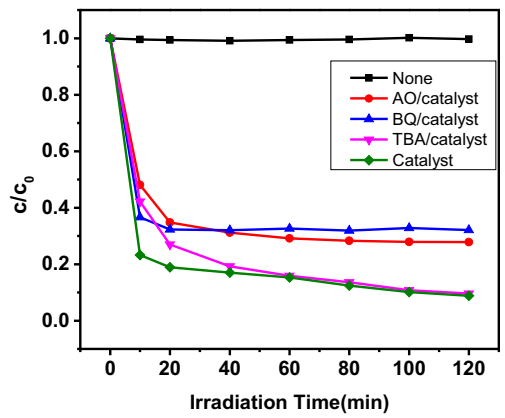

Fig. 9 Effect of various scavengers (AO, BQ and TBA) on the degradation of TC by Ag_3PO_4-PN, with TC concentration of 30 mg/L and catalyst dosage of 2 g/L

Photocatalyst stability and regeneration

The photocatalyst stability was assessed by the cyclic photocatalytic reaction experiments of TC by Ag_3PO_4-PN. The cycle experiments were carried out at the same conditions as usual degradation tests and Ag_3PO_4-PN catalyst was washed twice by distilled water and dried before reused. As shown in Fig. 10, the photodegradation activity of Ag_3PO_4-PN was availably held after five times loop experiments, indicating Ag_3PO_4-PN has relatively high stability under visible-light irradiation. Five degradation efficiencies of repeated experiments were 89, 85, 82, 77, and 74 %, respectively. Nevertheless, it was found that Ag_3PO_4 materials always

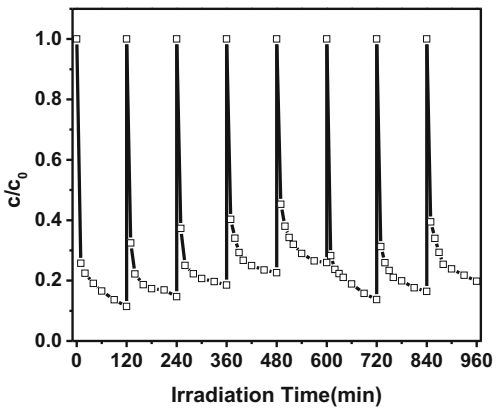

Fig. 10 Five times recycling runs of Ag_3PO_4-PN and three times degradation experiment of regenerative Ag_3PO_4-PN for the degradation of TC under visible-light irradiation. Each run of photocatalytic reaction lasted for 120 min (catalyst dosage = 1.0 g/L, TC concentration = 20 mg/L, pH = 4.3)

possessed photo-corrosion characteristics, and reductive elemental silver wrapped around the surface of Ag_3PO_4 catalyst may have a negative effect on the photo-absorption performance and photocatalytic activity of Ag_3PO_4, which prevented practical application of Ag_3PO_4 as a recyclable high-efficient photocatalyst [Yi et al. 2010].

A facile wet chemical-oxidation method was utilized to rejuvenate Ag_3PO_4-PN from weakly active Ag, which was previously reported by Wang and his coauthors. During the rejuvenation process, weakly active Ag can be oxidized by dropwise adding H_2O_2 into saturated PO_4^{3-} solution. While the acid environment of NaH_2PO_4 and H_3PO_4 aqueous solution can dissolve the Ag_3PO_4, and the fast decomposition of H_2O_2 will occur under strong alkaline condition of Na_3PO_4 solution, weaker alkaline Na_2HPO_4 was chosen as the source for PO_4^{3-} ions [Wang et al. 2012]. The photodegradation efficiency of TC by rejuvenated Ag_3PO_4-PN during three times recycling runs were 86, 84, and 80 %, respectively, indicating a successful rejuvenation of Ag_3PO_4, which greatly promotes the development of Ag_3PO_4 for practical applications.

Conclusion

A facile, environmental-friendly Ag_3PO_4-PN photocatalyst was successfully synthesized by a simple precipitation method at room temperature with the presence of $NH_3{\cdot}H_2O$ and PVP. The Ag_3PO_4-PN exhibits a superior photocatalytic activity compared to those of Ag_3PO_4-A, Ag_3PO_4-P, and Ag_3PO_4-N under visible-light irradiation. The enhancement of photocatalytic efficiency of Ag_3PO_4-PN is strongly dependent on the excellent photo-absorption capacity, sharp edges and corners, and synergistic effect of PVP and $NH_3{\cdot}H_2O$. The effect researches of reaction conditions indicated that the optimum condition were 2.0 g/L of catalyst dosage, 30 mg/L of TC solution concentration, and 5 of pH value of TC solution. Radical detection experiments indicate the h^+ and $\cdot O^{2-}$ are major active species in the degradation of TC by Ag_3PO_4-PN. TOC test and IC analysis indicate TC molecular was partially mineralized under the visible-light irradiation by Ag_3PO_4-PN. Moreover, photocatalyst stability and regeneration experiments exhibit a favorable stability and rejuvenation ability, suggesting a promising prospect of practical application of Ag_3PO_4 in the wastewater treatment.

References

Bandara J, Nadtochenko V, Kiwi J, Pulgarin C (1997) Dynamics of oxidant addition as a parameter in the modelling of dye mineralization (orange II) via advanced oxidation technologies. Water Sci Technol 35:87–93

Bertelli M, Selli E (2004) Kinetic analysis on the combined use of photocatalysis, H_2O_2 photolysis, and sonolysis in the degradation of methyl tert-butyl ether. Appl Catal B: Environ 52:205–212

Bertrand PA (1981) XPS study of chemically etched Gaas and Inp. J Vac Sci Technol 18:28–33

Bi YP, Ouyang SX, Umezawa N, Cao JY, Ye JH (2011) Facet effect of single-crystalline Ag_3PO_4 sub-microcrystals on photocatalytic properties. J Am Chem Soc 133:6490–6492

Daughton CG, Ternes TA (1999) Pharmaceuticals and personal care products in the environment: agents of subtle change? Environ Health Perspect 107:907–938

Ellis JB (2006) Pharmaceutical and personal care products (PPCPs) in urban receiving waters. Environ Pollut 144:184–189

Golovko O, Kumar V, Fedorova G, Randak T, Grabic R (2014) Seasonal changes in antibiotics, antidepressants/psychiatric drugs, antihistamines and lipid regulators in a wastewater treatment plant. Chemosphere 111:418–426

Guan XJ, Shi JW, Guo LJ (2013) Ag_3PO_4 photocatalyst: hydrothermal preparation and enhanced O_2 evolution under visible-light irradiation. Int J Hydrogen Energ 38:11870–11877

Guo XY, Chen CF, Yin SY, Huang LJ, Qin WP (2015) Controlled synthesis and photocatalytic properties of Ag_3PO_4 microcrystals. J Alloy Compd 619:293–297

Hua X, Teng F, Zhao YX, Xu J, Xu CY, Yang Y, Zhang QQ, Paul SS, Zhang Y, Chen MD, Zhao XD (2015) A new application of high-efficient silver salts-based photocatalyst under natural indoor weak light for wastewater cleaning. Water Res 81:366–374

Katsumata H, Taniguchi M, Kaneco S, Suzuki T (2013) Photocatalytic degradation of bisphenol A by Ag_3PO_4 under visible light. Catal Commun 34:30–34

Katsumata H, Sakai T, Suzuki T, Kaneco S (2014) Highly efficient photocatalytic activity of g-C_3N_4/Ag_3PO_4 hybrid photocatalysts through Z-scheme photocatalytic mechanism under visible light. Ind Eng Chem Res 53:8018–8025

Li M, Chen MD, Wang J, Teng F (2014) Branching growth of novel silver phosphate dendrites and the greatly improved photocatalytic activity by the active {110} facets. CrystEngComm 16:1237–1240

Liang QH, Ma WJ, Shi Y, Li Z, Yang XM (2012) Hierarchical Ag_3PO_4 porous microcubes with enhanced photocatalytic properties synthesized with the assistance of trisodium citrate. Cryst Eng Comm 14: 2966–2973

Lin YM, Li DZ, Hu JH, Xiao GC, Wang JX, Li WJ, Fu XZ (2012) Highly efficient photocatalytic degradation of organic pollutants by PANI-modified TiO_2 composite. J Phys Chem C 116:5764–5772

Liu YP, Wang JX, Lu HD, Li M, Chen P, Fang L (2014) Facile synthesis of visible-light-driven Ag_3PO_4 nanocrystals base on IP6 micelles. Catal Commun 55:65–69

Mahmoodi NM, Arami M, Zhang J (2011) Preparation and photocatalytic activity of immobilized composite photocatalyst (titania nanoparticle/activated carbon). J Alloy Compd 509:4754–4764

Martins VV, Zanetti MOB, Pitondo-Silva A, Stehling EG (2014) Aquatic environments polluted with antibiotics and heavy metals: a human health hazard. Environ Sci Pollut R 21:5873–5878

Ortiz de Garcia SA, Pinto Pinto G, Garcia-Encina PA, Irusta-Mata R (2014) Ecotoxicity and environmental risk assessment of pharmaceuticals and personal care products in aquatic environments and wastewater treatment plants. Ecotoxicology 23:1517–1533

Sakthivel S, Neppolian B, Shankar MV, Arabindoo B, Palanichamy M, Murugesan V (2003) Solar photocatalytic degradation of azo dye: comparison of photocatalytic efficiency of ZnO and TiO_2. Sol Energ Mat Sol C 77:65–82

Teng F, Liu ZL, Zhang A, Li M (2015) Photocatalytic performances of Ag_3PO_4 polypods for degradation of dye pollutant under natural indoor weak light irradiation. Environ Sci Technol 49:9489–9494

Ternes TA, Joss A, Siegrist H (2004) Peer reviewed: scrutinizing pharmaceuticals and personal care products in wastewater treatment. Environ Sci Technol 38:392–399

Wang H, Bai YS, Yang JT, Lang XF, Li JH, Guo L (2012) A facile way to rejuvenate Ag_3PO_4 as a recyclable highly efficient photocatalyst. Chem Eur J 18:5524–5529

Wang J, Teng F, Chen MD, Xu JJ, Song YQ, Zhou XL (2013) Facile synthesis of novel Ag_3PO_4 tetrapods and the {110} facets-dominated photocatalytic activity. CrystEngComm 15:39–42

Wang J, Lou SQ, Sun P, Wang LL, Teng YR, Chen MD, Teng F (2014a) Surface control and photocatalytic activity of branched silver orthophosphate dendrites. ChemCatChem 6:2021–2027

Wang K, Xu J, Hua X, Li N, Chen MD, Teng F, Zhu YF, Yao WQ (2014b) Highly efficient photodegradation of RhB–MO mixture dye wastewater by Ag_3PO_4 dodecahedrons under acidic condition. J Mol Catal A Chem 393:302–308

Wang LL, Li N, Zhang QY, Lou SQ, Zhao YX, Chen MD, Teng F (2014c) A innovative glycine complexing approach to silver phosphate myriapods with improved photocatalytic activity. CrystEngComm 16:9326–9330

Wang HQ, Ye ZF, Liu C, Li JZ, Zhou MJ, Guan QF, Lv P, Huo PW, Yan YS (2015) Visible light driven Ag/Ag_3PO_4/AC photocatalyst with highly enhanced photodegradation of tetracycline antibiotics. Appl Surf Sci 353:391–399

Wu AP, Tian CG, Chang W, Hong Y, Zhang Q, Qu Y, Fu HG (2013) Morphology-controlled synthesis of Ag_3PO_4 nano/microcrystals and their antibacterial properties. Mater Res Bull 48:3043–3048

Xiao X, Hao R, Zuo XX, Nan JM, Li LS, Zhang WD (2012) Microwave-assisted synthesis of hierarchical $Bi_7O_9I_3$ microsheets for efficient photocatalytic degradation of bisphenol-A under visible light irradiation. Chem Eng J 209:293–300

Yang ZM, Liu YY, Xu L, Huang GF, Huang WQ (2014) Facile shape-controllable synthesis of Ag_3PO_4 photocatalysts. Mater Lett 133: 139–142

Yi ZG, Ye JH, Kikugawa N, Kako T, Ouyang SX, Stuart-Williams H, Yang H, Cao JY, Luo WJ, Li ZS, Liu Y, Withers RL (2010) An orthophosphate semiconductor with photooxidation properties under visible-light irradiation. Nat Mater 9:559–564

Zhang Y, Xiong Y, Tang Y, Wang Y (2013) Degradation of organic pollutants by an integrated photo-Fenton-like catalysis/immersed membrane separation system. J Hazard Mater 244:758–764